INTERNATIONAL JOURNAL OF INTEGRATED ENGINEERING
ISSN: 2229-838X e-ISSN: 2600-7916

IJIE

Vol. 15 No. 5 (2025) 98-114
https://publisher.uthm.edu.my/ojs/index.php/ijie

An Antilock Braking-Guided Steering Mathematical Modelling with Integrated Automatic Control in Vehicles and Its Evaluation

Andika Wisnujati[1]*, Hsing-Chung Chen[2,3], Agung Mulyo Widodo[4], Chi-Wen Lung[5,6]

[1] *Universitas Muhammadiyah Yogyakarta, Department of Automotive Engineering Technology*
Brawijaya Street, Tamantirto, Kasihan, Bantul, 55183, INDONESIA
[2] *Asia University, Department of Computer Science and Information Engineering*
Liufeng Road, Wufeng Districr, Taichung City, 413, TAIWAN
[3] *China Medical University, Department of Medical Research*
Xueshi Rd, North District, Taichung City, 404, TAIWAN
[4] *Universitas Esa Unggul, Department of Computer Science*
Arjuna Utara No.9, Duri Kepa, Daerah Khusus Ibukota Jakarta 11510, INDONESIA
[5] *Asia University, Department of Creative Design*
Liufeng Road, Wufeng Districr, Taichung City, 413, TAIWAN
[6] *University of Illinois, Department of Rehabilitation Engineering*
Urbana-Champaign, Champaign, Illinois, 61820, USA

*Corresponding Author: andikawisnujati@umy.ac.id
DOI: https://doi.org/10.30880/ijie.2025.17.05.009

Article Info

Received: 24 July 2024
Accepted: 15 May 2025
Available online: 30 August 2025

Keywords

Antilock braking guided steering (AB-GS) system, stopping distance, PID controller, slip control

Abstract

In the cars industry, to control slip rate from wheels and help drivers to avoid accidents on road, an integrated antilock braking and guided steering (AB-GS) system has been developed for vehicles especially cars. The brake and steering system are devices to slow down or stop the movement of the wheels on the vehicle and have ease of control and directional stability. Because the wheels are slowed down, the vehicle's motion automatically slows down. The lost kinetic energy is con-verted into heat due to friction. The three purposes of the AB-GS brake controller are to reduce stopping time, limit slip ratio, and improve control system performance (by reducing time ratio and overshoot). For that, we build a model based on the equations of motion, which are affected by forces and moments for each axis. This research utilized MATLAB as a tool for modeling the system dynamics and simulating the performance of the AB-GS brake controller. In the ABS system, there is an influence of force or moment towards the lateral (X), longitudinal (Y), and vertical (Z) axes. At the time of braking, there will be a change in directional force (X, Y, and Z) as well as moments that affect the direction of rolling motion, yaw and pitching. When braking forcefully, it is equally important to maintain vehicle stability and steering control as it is to minimize stopping distance. Changes in motion along the Z-axis, as well as moments affecting yaw and roll, are not considered in this study. Then, from the system's equations of motion, we can control it using PID control. By controlling the system, it is expected to prevent the vehicle from experiencing sudden locking, which can result in overturning. In this research, control performance was also tested

This is an open access article under the CC BY-NC-SA 4.0 license.

using PID, which can improve vehicle driving ability, safety, and operating stability. To fully maintain vehicle direction stability, its integration with other control systems is needed. Simulation results validating the integrated antilock-braking and steering system not only obtain better optimal braking distances and excellent predictability but also show that the integrated control system outperforms the stand-alone braking and steering system.

1. Introduction

During the 20th century, a range of electrically controlled methods and systems, including but not limited to anti-lock braking systems and active suspension systems, were developed, and refined to enhance vehicle maneuverability, safety, and operational stability. Nonetheless, many of these control subsystems operate in isolation from each other. Traffic accidents are one of the leading causes of injuries and fatalities all over the world [1]. Most today's crashes in Indonesia can be attributed to driver error (61%), which primarily consists of recognition and decision making (30%), followed by performance errors (9%) and fatality rate in South-East Asian countries (12.2 per 100,000 people) [2]. In fact, the sport utilities vehicle (SUV) control system is a complex system, and the vehicle's performance is heavily dependent not only on each subsystem, but also on the relationships between these subsystems [3]. Despite exhibiting a higher inclination towards overdrafts, reduced maneuverability, and lower fuel efficiency compared to other segments of passenger vehicles, SUVs dominate the global market share for such cars, with their popularity continually increasing. As vehicle technology has progressed, the functions of automobiles have evolved as well. A notable transformation can be observed in braking systems, which not only safeguard the vehicle but also empower the driver to respond effectively in emergency braking situations. This evolution is attributed to factors such as extended wheelbases, broader track, and elevated center of gravity. Highway vehicles could move in all directions without being restricted by lanes or tracks in accordance with orders from the vehicle driver.

The AB-GS primary function is to independently control the brake torque of the four wheels to prevent them from locking. Most of these control subsystems, however, operate independently [4]. In fact, the control system of a vehicle is a complicated system whose performance depends not only on the individual subsystems but also greatly on the relationships among these subsystems. AB-GS typically enhances vehicle safety by minimizing lateral wheel slips when encountering intense braking conditions [5-6]. When sliding on the road, the friction force on the locked wheel is usually much lower. When braking, if one or more vehicle wheels lock (begin to slip), several consequences occur, including increased braking distances, loss of steering control, and tire wheel abnormalities. These are unfavorable circumstances. AB-GS, traction control systems, and other safety and reliability features are standard in modern automobiles. A well-functioning AB-GS control system should effectively maintain wheel slip within an ideal range suitable for prevailing road conditions, thereby averting wheel lock-up during braking maneuvers [7]. Various methods, including robust control, describing function analysis, sliding mode control, among others, have been effectively utilized in AB-GS control strategies [8]. The vehicle's traction control can be taken over entirely or partially by the autonomous ABS system [9]. The AB-GS, on the other hand, has strong nonlinear properties [10]. On the contrary, a dynamic four-wheel vehicle model that considers the changing normal load on the wheels and generates suitable lateral forces is ideal for designing a reliable brake system [11]. The main objective of the AB-GS is to swiftly decelerate a vehicle while preserving its maneuverability during emergency braking maneuvers. Its principal aim is to enhance brake efficiency, steering response, and overall driving stability. AB-GS has become a mandatory safety feature in nearly every country worldwide [6,12].

A steering system is an apparatus enabling the alteration of a motor vehicle's direction of motion. An integrated steering system, therefore, comprises multiple interconnected components that work together. In the context of this study, integration denotes the merging of systems that traditionally operate independently with mutual agreement [13]. As a result, any subsystem that is used will be developed with the other in consciousness. This will be done to optimize area, resources, and performance. This study focuses on the optimal control of both braking and steering systems for a vehicle undergoing hard braking while turning. This presents a novel situation where enhanced braking effectiveness is sought alongside improved lateral stability. Through this approach, traditional ABS can achieve directional stability with only a slight decrease in maximum braking force [14]. Hence, a learning control strategy becomes essential to enhance its performance gradually, adapting to diverse road conditions. Alongside passive suspension, recent literature explores numerous endeavors to integrate road classification with semi-active vehicle suspension, aiming to enhance both ride comfort and handling [10,15]. Because the primary goal of a semi-active suspension system is to achieve a good balance of suspension system and ability to handle, awareness of the road conditions gives guidance on the implementation of control parameters to modify performance of the system [16-17]. Semi-active suspension refers to a form of vehicle suspension that adjusts the damping force of the shock absorber in reaction to the continuously varying conditions

of the road. It serves as a close approximation to active suspension, featuring a shock absorber with adjustable damping force [17-18].

In response to wheel decline and slip, ABS is activated and deactivated. It is used in modern automobiles to improve safety and consistency [11]. It is primarily an engaged protective measure that is now installed in most automobiles and is responsible for preventing the wheels from locking during hard braking [19]. In the automotive industry, ABS is a well-known safety feature. To forecast how a vehicle will react when doing the maneuvers the driver wants, its characteristics become a very important item for modelling. Vehicles that are safe and comfortable according to the requirements can be designed using the results of vehicle dynamic system modelling.

The PID algorithm is presumed to regulate the ABS system of the examined vehicle, chosen for its straightforwardness and minimal processing demands [20-21]. A review of ABS simulation outcomes indicates that the proportional electro-hydraulic brake can notably diminish braking distance and address hydraulic pressure fluctuations experienced on diverse road surfaces. The investigation suggests the viability of employing this proportional pressure control valve in commercial brake systems as a substitute for conventional solenoid valves [22].

These studies restricted the development of an automatic brake control system using adaptive PID. When an obstacle ahead is detected by the controller system, an automatic brake control system will be designed to decrease velocity from a predetermined speed. Thus, this research contributes as follows:

• Proposes a control design for integrating the front steering and braking systems to maintain vehicle stability while enhancing lateral responsiveness during emergency collision avoidance

• Simulate the mathematical modelling of AB-GS designed and compared using MATLAB/Simulink. In this study, an adaptive PID controller method was used to tune the proportional, integral, and derivative control parameters

• This controller's objectives for the AB-GS brake are to reduce stopping time, limit slip ratio, and improve the performance controlling system (by reducing settling time and overshoot). The simulation results demonstrated that our objectives have been achieved.

The goal of the most recent study on the interaction between the steering system and the antilock braking system (ABS) in automobiles is to maximize vehicle safety. The goal of this research is to create a system that can better control a vehicle during emergency braking circumstances by coordinating the responses of the steering system and ABS. The objectives of this integration are to reduce stopping distances, improve stability, and distribute brake power more evenly across the wheels. This research has the potential to improve the dependability of vehicle responses to unexpected braking, lowering the likelihood of accidents, and raising road user safety by merging data from ABS sensors and the steering system. These developments reflect the auto industry's continuous efforts to combine various technologies to improve the general performance and safety of vehicles.

2. Systematic Modelling

Systematic modelling in the context of an Antilock Braking System (ABS) refers to the process of creating a structured representation of the ABS and its components. This modelling approach aims to understand, analyse, and design the ABS in a methodical and organized manner. Systematic modelling involves breaking down the complex system into smaller, more manageable parts, and then defining their interconnections and behaviours [23].

Despite significant advancements in automotive safety systems, a notable research gap exists in the integration of antilock braking systems (ABS) with steering mechanisms to enhance vehicle control and stability under emergency braking conditions. While ABS technology has been widely adopted to prevent wheel lock-up and maintain steering control during braking, current systems primarily focus on braking performance alone, without seamless coordination with steering inputs. Integrating ABS with steering systems could potentially offer enhanced maneuverability and collision avoidance capabilities by optimizing braking force distribution and steering response simultaneously. However, the development of such integrated systems poses technical challenges related to sensor fusion, real-time control algorithms, and vehicle dynamics modelling, necessitating further research to explore the feasibility, effectiveness, and implementation challenges of integrating ABS with steering for improved vehicle safety and performance.

2.1 Vehicle Dynamic Model

A passenger longitudinal vehicle model is comprising a single sprung mass that represents the vehicle body. We use the coordinate system to analysis the vehicle motion as described in Fig. 1. In vehicle dynamics, the equations of motion are typically represented as a set of x, y, and z coordinate system equations centered on the vehicle's centre of gravity (CG).

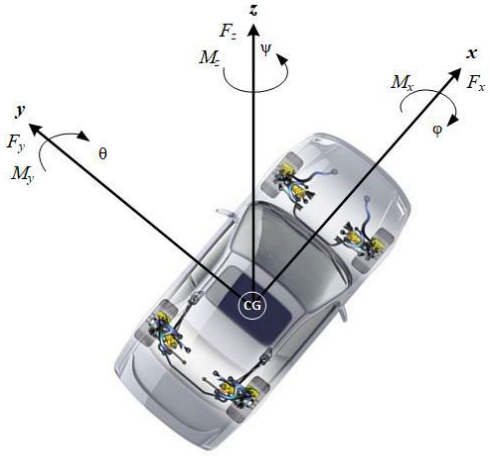

Fig. 1 *Vehicle in a coordinate system*

We use the coordinate system to analysis the vehicle motion as described in Fig. 1. For convenience, vehicle motion is defined using the right-hand rule coordinate system [24], the coordinates are defined as follows. The vehicle has a fixed coordinate system on the vehicle itself using the right-hand rule. However, the movement of the vehicle must be defined into another coordinate system that is fixed or does not change with respect to the vehicle, such a coordinate system is called a global coordinate system [25-26]. This global coordinate system is used to evaluate the trajectory or trajectory of the vehicle. Most researchers usually use a two-degree-of-freedom (DOF) model to investigate the dynamic characteristics of a vehicle, which differs from the precise steering condition of the vehicle [27].

The general equations for resulting force and moment which act on a vehicle are presented by the following Eq. (1).

$$F = F_x\vec{i} + F_y\vec{j} + F_z\vec{k}$$
$$M = M_x\vec{i} + M_y\vec{j} + M_z\vec{k} \quad (1)$$

Int. Journal of Integrated Engineering Vol. 17 No. 5 (2025) p. 98-114

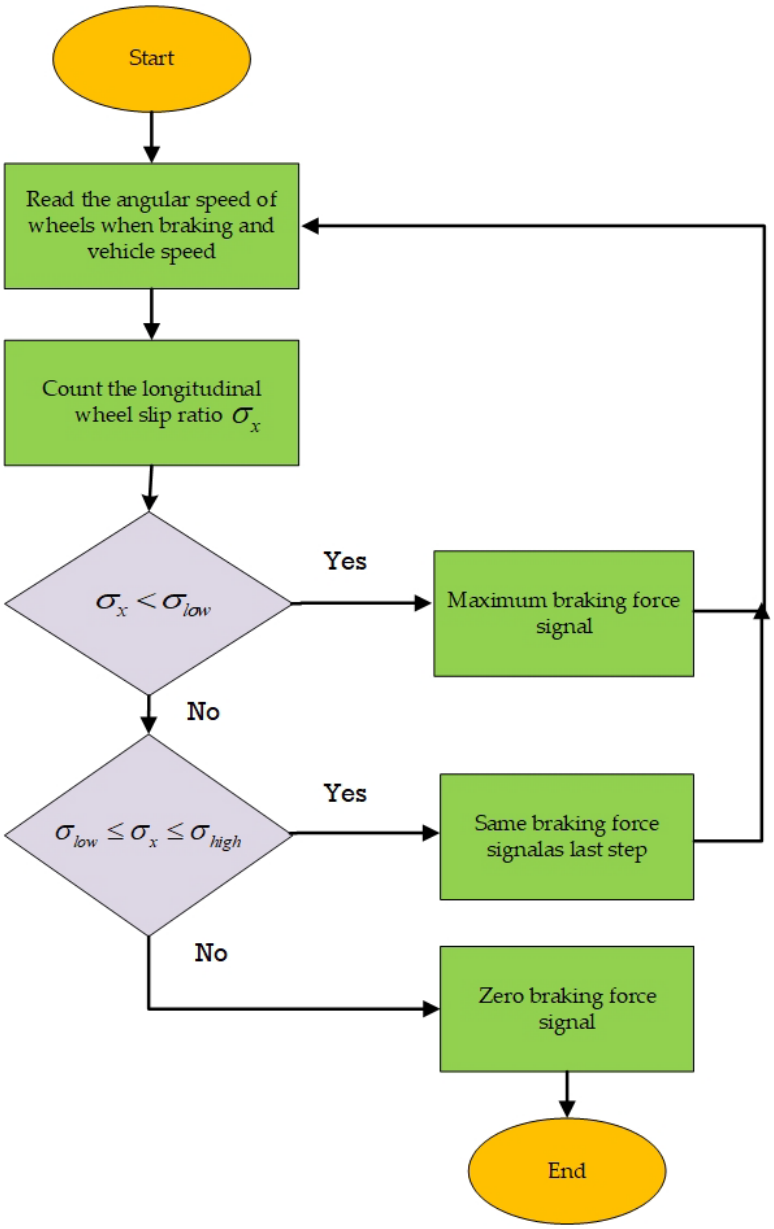

Fig. 2 *System architecture*

Each wheel can rotate around its axis, and all four wheels can move in the same direction [1]. Our method is illustrated in Fig. 2, which describes the whole system architecture. The dynamic bicycle model takes into consideration 2D planar motion, including rotation around the reference frame's *Z* axis (yaw) and translation along the *X* and *Y* axes (longitudinal/lateral). In some circumstances, such as path tracking, the effort is reduced to regulating lateral dynamics and yaw motion, resulting in a 2-DoF model [28-29]. The Vehicle Body 2DOF block employs a rigid two-axle vehicle body model to ascertain longitudinal, lateral, and yaw movements. It considers factors such as body mass, aerodynamic drag, and weight distribution between the axles, which are influenced by acceleration and steering.

Newton's principles are applied to the straightforward bicycle model [30-31] in Fig. 3 to provide the following model Eq. (2) and Eq. (3):

$$\sum F_x = m \,.\, a_x \tag{2}$$

$$\sum F_y = m \,.\, a_y \tag{3}$$

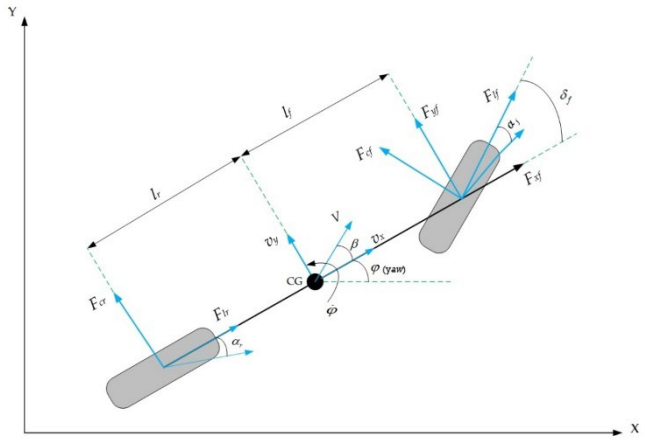

Fig. 3 *Single track bicycle*

In such cases, the lateral tire forces can be expressed as follows in Eq. (4):

$$\begin{aligned} F_{cf} &= C_f.\alpha_f \\ F_{cr} &= C_r.\alpha_r \end{aligned} \tag{4}$$

The steering angles F_{cf} and F_{cr} for the front and rear wheels are the model's inputs, however as most cars can only be turned through the front wheel, r is typically null. The distances between the wheel axles and the center of gravity (lf and lr) are the only two factors needed to identify in the kinematic model, making it simple to apply the same controller to other vehicles with varying wheelbases. The initial study utilized the vehicle's bicycle model, which does not incorporate roll, pitch, or heave movements, and it does not address suspension dynamics [32]. As a result, this model cannot accurately represent load transfer during maneuvering and braking. A vehicle suffers two motions, i.e., translation motion and rotation motion. The translation-al speed of the vehicle could be defined in Eq. (5).

$$V_T = V_x\hat{\imath} + V_y\hat{\jmath} + V_z\hat{k} \tag{5}$$

Furthermore, it could be defined as the angular momentum and angular velocity of the vehicle as follows in Eq. (6) and Eq. (7).

$$H = H_x\hat{\imath} + H_y\hat{\jmath} + H_z\hat{k} \tag{6}$$

$$\omega = \omega_x\hat{\imath} + \omega_y\hat{\jmath} + \omega_z\hat{k} \tag{7}$$

To derive the dynamic model of vehicle, we could be using the motion equation of vehicles regarding the Newton's second law in Eq. (8).

$$\sum F = m\left\{\frac{d}{dt}V_T + (\omega \times V_T)\right\} \tag{8}$$

We could be rewritten Equation (8) as Equation (9) as follows.

$$\begin{aligned} \sum F_x\hat{\imath} &= m\left(\dot{V}_x + \left(\omega_y V_z - \omega_z V_y\right)\right)\hat{\imath} \Rightarrow \sum F_x = m\left(\dot{V}_x + \left(\omega_y V_z - \omega_z V_y\right)\right) \\ \sum F_y\hat{\jmath} &= m\left(\dot{V}_y + \left(\omega_z V_x - \omega_x V_z\right)\right)\hat{\jmath} \Rightarrow \sum F_y = m\left(\dot{V}_y + \left(\omega_z V_x - \omega_x V_z\right)\right) \\ \sum F_z\,\hat{k} &= m\left(\dot{V}_z + \left(\omega_x V_y - \omega_y V_x\right)\right)\hat{k} \Rightarrow \sum F_z = m\left(\dot{V}_z + \left(\omega_x V_y - \omega_y V_x\right)\right) \end{aligned} \tag{9}$$

Since it is assumed that there is no motion of sprung mass, then we neglect the forces of z axis ($\sum F_z = 0$). By considering the lateral force equilibrium, neglecting the road set point, and implementing Newton's second law

[33] of motion along the y axis yields the equation for the vehicle's lateral movement then Eq. (9) could be mentioned as in Eq. (10).

$$\begin{aligned}\sum F_y &= m\left(\dot{V}_y + \omega_z V_x - \omega_x V_z\right) = m\left(\left(\dot{V}_y + \Delta\dot{V}_y\right) + (\omega_z + \Delta\omega_z)(V_x + \Delta V_x) - (\omega_x + \Delta\omega_x)(V_z + \Delta V_z)\right)\\ \sum F_y &= m\left(\Delta\dot{V}_y + V_x\Delta\omega_z + \omega_z\Delta V_x + \Delta\omega_z\Delta V_x - V_z\Delta\omega_x - \omega_x\Delta V_z - \Delta\omega_x\Delta V_z\right)\end{aligned} \tag{10}$$

It is assumed all the initial variables have zero value then Eq. (10) could be written as Eq. (11).

$$\sum F_y = m\left(\Delta\dot{V}_y + \Delta\omega_z\Delta V_x\right) \tag{11}$$

Next, the lateral forces are the total forces at front and rear of vehicle, then it could be mentioned in Eq. (12) as follows.

$$\begin{aligned}&F_{yr} = F_{cr}\cos\delta_r\,;F_{yf} = F_{cf}\cos\delta_f\\ &\sum F_y = F_{yf} + F_{yr} = F_{cf}\cos\delta_f + F_{cr}\cos\delta_r\\ &F_{cf}\cos\delta_f + F_{cr}\cos\delta_r = m\Delta\dot{V}_y + \Delta\omega_z\Delta V_x\end{aligned} \tag{12}$$

It is defined $F_{cf} = C_{cf}\left(\delta_f - tan^{-1}\left(\frac{\Delta V_y + l_f\Delta\omega_z}{\Delta V_x}\right)\right)$ is the lateral tire forces of the front and $F_{cr} = C_{cr}\left(\delta_r - tan^{-1}\left(\frac{\Delta V_y + l_r\Delta\omega_z}{\Delta V_x}\right)\right)$ is rear wheels respectively. So, Eq. (12) could be written as Eq. (13).

$$\begin{aligned}&2C_{cf}\left(\delta_f - tan^{-1}\left(\frac{\Delta V_y + l_f\Delta\omega_z}{\Delta V_x}\right)\right)cos\,\delta_f + 2C_{cr}\left(\delta_r - tan^{-1}\left(\frac{\Delta V_y - l_r\Delta\omega_z}{\Delta V_x}\right)\right)\\ &= m\Delta\dot{V}_y + \Delta\omega_z\Delta V_x\end{aligned} \tag{13}$$

To simplify the derivation, we assume small angle variations in the steered angle δ. Based on this assumption, we linearized the $cos(\delta)$about an operating region around $\delta = 0$such that $cos(\delta) \simeq 1$. The exact lateral force balance is determined as in after determining the specifications for the front and rear tires, ignoring the road bank angle and using Newton's second law of motion along the y-axis could be stated in Eq. (14).

$$\dot{V}_y = \frac{2C_{\alpha f}\delta_f}{m} - \left(\frac{2C_{\alpha f} + 2C_{\alpha r}}{mV_x}\right)V_y + \left(\frac{2C_{\alpha r}l_r - 2C_{\alpha f}l_f}{mV_x} - V_x\right)\omega_z \tag{14}$$

Furthermore, according to the moment balance of a single-track bicycle is described in Figure 3, it could be derived the torque at the vehicle center of mass in Eq. (15).

$$\begin{aligned}M_x &= I_{xx}\dot{\omega}_x - I_{xz}\left(\dot{\omega}_z + \omega_x\omega_y\right) + \left(I_{zz} - I_{yy}\right)\omega_y\omega_z\\ M_y &= I_{yy}\dot{\omega}_y + I_{xz}\left(\omega_x^2 - \omega_y^2\right) + (I_{xx} - I_{zz})\omega_x\omega_z\\ M_z &= I_{zz}\dot{\omega}_z - I_{xz}\left(\dot{\omega}_x - \omega_y\omega_z\right) + \left(I_{yy} - I_{zz}\right)\omega_x\omega_y\end{aligned} \tag{15}$$

By neglecting the torque toward x and y axis and all of the initial values are zero, then Eq. (15) could be stated as Eq. (16).

$$\begin{aligned}M_z &= 2l_fC_{\alpha f}\delta_f - \left(\frac{2C_{\alpha f}l_f - 2C_{\alpha r}l_r}{V_x}\right)V_y + \left(\frac{2C_{\alpha f}l_f^2 - 2C_{\alpha r}l_r^2}{V_x}\right)\omega_z\\ I_{yy}\dot{\omega}_z + I_{xz}\omega_y\omega_z &= 2l_fC_{\alpha f}\delta_f - \left(\frac{2C_{\alpha f}l_f - 2C_{\alpha r}l_r}{V_x}\right)V_y + \left(\frac{2C_{\alpha f}l_f^2 - 2C_{\alpha r}l_r^2}{V_x}\right)\omega_z\\ I_{zz}\dot{\omega}_z &= 2l_fC_{\alpha f}\delta_f - \left(\frac{2C_{\alpha f}l_f - 2C_{\alpha r}l_r}{V_x}\right)V_y + \left(\frac{2C_{\alpha f}l_f^2 - 2C_{\alpha r}l_r^2}{V_x}\right)\omega_z - I_{xz}\omega_y\omega_z\\ \dot{\omega}_z &= \frac{2l_fC_{\alpha f}\delta_f}{I_{zz}} - \left(\frac{2C_{\alpha f}l_f - 2C_{\alpha r}l_r}{I_{zz}V_x}\right)V_y + \left(\frac{2C_{\alpha f}l_f^2 - 2C_{\alpha r}l_r^2}{I_{zz}V_x}\right)\omega_z - \frac{I_{xz}\omega_y\omega_z}{I_{zz}}\end{aligned} \tag{16}$$

The longitudinal motion of the vehicle as well as the rotational dynamics of the four wheels are used in the design of the wheel slip controller as follows in Eq. (11) and Eq. (12). As we know, the function of steering systems is:

- Should enable the driver to regulate the vehicle along a desired path.
- Should enable the control of the vehicle's trajectory under normal and emergency conditions.
- Critical system to ensure proper handling of the vehicle.

The forces suffer on front wheel is described as follows in Eq. (17):

$$\dot{V}_x = \frac{2F_x \cos\delta_f}{m} - \frac{2C_{\alpha_f}\delta_f}{mV_x} + \frac{2C_{\alpha r}\delta_r \sin\delta_f}{mV_x} + \frac{2C_{\alpha_f}V_y}{mV_x} - \frac{2C_{\alpha r}V_y \sin\delta_f}{mV_x} + \frac{2C_{\alpha_f}l_f\omega_z}{mV_x} - \frac{2C_{\alpha r}l_r\omega_z \sin\delta_f}{mV_x} \tag{17}$$

where F_x is the longitudinal force.

2.2 Half Car Model

The suspension model for the vehicle is constructed based on a vibrational model incorporating the car's suspension and tires with a 2-degree-of-freedom (2-DOF) setup, representing a system comprising masses (both sprung and unsprung), springs, and dampers. In the context of vehicles, 2-DOF typically refers to the ability of the vehicle to move in two independent directions, such as forward/backward and left/right [34]. This term is often used in discussions of vehicle dynamics and control. When the vehicle is subjected to dynamics, the tire loads can be calculated in real time (load transfer and aerodynamics). DOFs are depicted in Fig. 4 as follows.

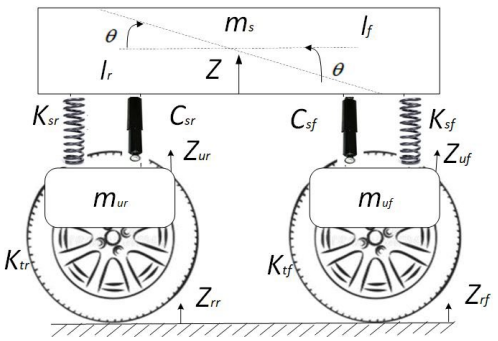

Fig. 4 *Half car model for vehicle suspension*

The equations of motion for this 2-DOF half-car model are as follows in Eq. (18) and Eq. (19). According to Fig. 4., in the *x*-*z* field, the vehicle body sprung mass is described as follows.

$$\begin{aligned}\sum F_z &= m_s\left(\dot{V}_z + \left(\omega_x V_y - \omega_y V_x\right)\right)\\ &= m_s\left(\left(\dot{V}_z + \Delta\dot{V}_z\right) + \left((\omega_x + \Delta\omega_x)(V_y + \Delta V_y) - (\omega_y + \Delta\omega_y)(V_x + \Delta V_x)\right)\right)\\ &2\left(F_{zf} + F_{z_r}\right) - 2K_{sf}\left(z - l_f\theta - z_{uf}\right) - 2K_{sr}(z + l_r\theta - z_{ur}) - 2C_s + \left(V_z - l_f\omega_y - V_{z_{uf}}\right)\\ &\quad - 2C_{sr}\left(V_z + l_r\omega_y - V_{z_{ur}}\right)\\ &= m_s\left(\dot{V}_z - \omega_y V_x\right)\end{aligned} \tag{18}$$

where l_f and l_r is the distance between front and rear suspension. Symbol z, z_{uf} and z_{ur} are the displacement of sprung mass, front sprung mass, and rear sprung mass, respectively.

Whereas the unsprung mass is described as Eq. (19) for front side and Eq. (20) for rear side.

$$\begin{aligned}&-2F_f + 2K_{sf}\left(z - l_f\theta - z_{uf}\right) + 2C_{sf}\left(\dot{z} - l_f\dot{\theta} - \dot{z}_{uf}\right) - 2K_{tf}\left(z_{uf} - z_{rf}\right)\\ &= m_{uf}\left(\dot{V}_{x_{uf}} + \omega_{y_{uf}}V_{uf} - \omega_{z_{uf}}V_{y_{uf}}\right)\end{aligned} \tag{19}$$

$$\begin{aligned}&-2F_r + 2K_{sr}(z + l_r\theta - z_{ur}) + 2C_{sr}(z + l_r\theta - z_{ur}) - 2K_{tr}(z_{ur} - z_{rr})\\ &= m_{ur}\left(\dot{V}_{x_{ur}} + \omega_{y_{ur}}V_{ur} - \omega_{z_{ur}}V_{y_{ur}}\right)\end{aligned} \tag{20}$$

Int. Journal of Integrated Engineering Vol. 17 No. 5 (2025) p. 98-114

2.3 Load Transfer Vehicle

Load transfer in wheeled vehicles refers to the quantifiable variation in the load carried by various wheels during acceleration (both longitudinally and laterally) [2]. This covers both braking and deceleration, which is an acceleration that is happening more slowly.

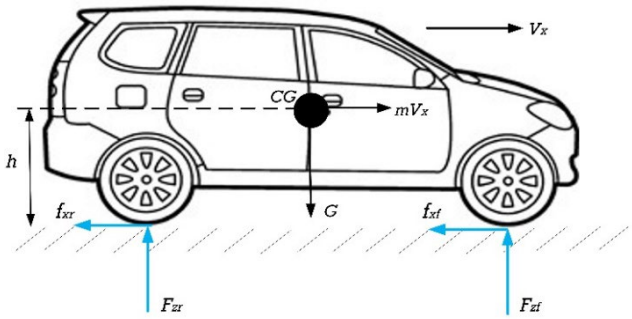

Fig. 5 *Vehicle longitudinal model*

The vehicle motion model computes vehicle dynamics and can be utilized to derive parameters such as speed, slip, and braking distance during deceleration. Subsequently, a longitudinal vehicle model and a single-wheel model are delineated in Fig. 4 and Fig. 5. As depicted in Fig. 5, the vehicle is assumed to decelerate on a level, straight road surface, with a constant coefficient of friction [27]. Factors such as air resistance and rolling resistance are disregarded. Utilizing Newton's Second Law, the forces acting on the front wheel can be elucidated as detailed in Eq. (21).

$$\begin{aligned} \sum F_{x_{uf}} &= m_{uf}\left(\dot{V}_{x_{uf}} - \omega_{y_{uf}} V_{x_{uf}}\right) \\ m_{uf}\left(\dot{V}_{x_{uf}} - \omega_{y_{uf}} V_{x_{uf}}\right) &= -f_{x_{uf}} \\ \dot{V}_{x_{uf}} &= -\frac{f_{x_{uf}}}{m_{uf}} + \omega_{y_{uf}} V_{x_{uf}} \end{aligned} \tag{21}$$

Next, the total torque suffers to front wheel is shown in Equation (22).

$$\dot{\omega_{y_{uf}}} = \frac{f_{x_f} r}{m_{uf}} - \frac{\tau_{b_f}}{m_{uf}} \tag{22}$$

whereas the forces and total torque suffer to rear wheel could be stated as follows in Eq. (23) to Eq. (25).

$$\dot{V}_{x_r} = -\frac{f_{x_{ur}}}{m_{ur}} + \omega_{y_{ur}} V_{x_{ur}} \tag{23}$$

$$\dot{\omega_{y_{ur}}} = \frac{f_{x_r} r}{m_{ur}} - \frac{\tau_{b_r}}{m_{ur}} \tag{24}$$

$$F_{zr} = \frac{G l_f - m V_x H}{\left(l_f + l_r\right)} \tag{25}$$

where, $f_{f_r} = f_{x_r} = \mu F_{zf} = \mu F_{zr}$ and $F_z = F_{zf} + F_{zr}$

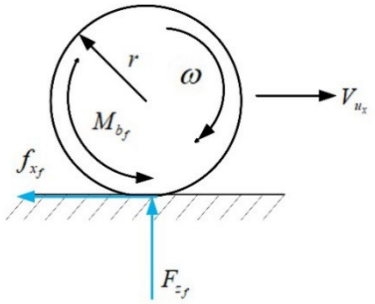

Fig. 6 *Single wheel braking model*

The importance of tire force is such that it affects how accurate a simulation is. The tire model requires consideration of the influence of tire vertical force on longitudinal and lateral forces as well as their interaction.

The Burckhardt model is utilized to forecast the longitudinal force of a vehicle in deceleration scenarios. This is achieved by employing mathematical deformation and simulation analyses that are grounded on the magic formula model. The Burckhardt equation [3-4], which is frequently used to represent tire forces, is developed using a similar process and uses μ as a function of both wheel slip (λ) and vehicle velocity (v), that shown in Eq. (26).

$$\mu(\lambda, v) = \left[C_1\left(1 - e^{-C_2\lambda}\right) - C_3\lambda\right]e^{-C_4\lambda v} \tag{26}$$

where C_1 is the maximum value of the friction curve, C_2 is the form of the friction curve, C_3 is the difference between the maximum value and the value at $\lambda = 1$, and C_4 is the value representing the characteristics of the road.

Table 1 *Friction parameters*

Surface parameters	C_1	C_2	C_3	C_4
Asphalt-dry	1.029	17.16	0.523	0.035
Asphalt-wet	0.857	33.822	0.347	0.035

The longitudinal force diminishes in response to the side slip angle. The foundation for ABS brakes is this physical occurrence since it safeguards the vehicle's steering system and lateral stability by minimizing high longitudinal slip values while braking. Operating with wheel slip values to the right of any peak in the friction curve results in rapid slip dynamics and open loop instability, making manual control challenging.

3. Pid Controller

Proportional, integral, and derivative (PID) controllers continue to be widely utilized in industrial applications due to their simplicity and robustness, despite advancements in control strategies. In addition to providing feedback, PID controllers can eliminate steady-state errors through integral action and predict the future via derivative action [5]. In Aksjonov [6], various PID controller structures and tuning rules are described. The Ziegler-Nichols tuning rule is the predominant and extensively employed method in PID applications. The system consists of three components: proportional, integral, and derivative [35]. Design criteria can be satisfied by modifying the parameters of controllers in the control system K_P, K_i and K_d.

Int. Journal of Integrated Engineering Vol. 17 No. 5 (2025) p. 98-114

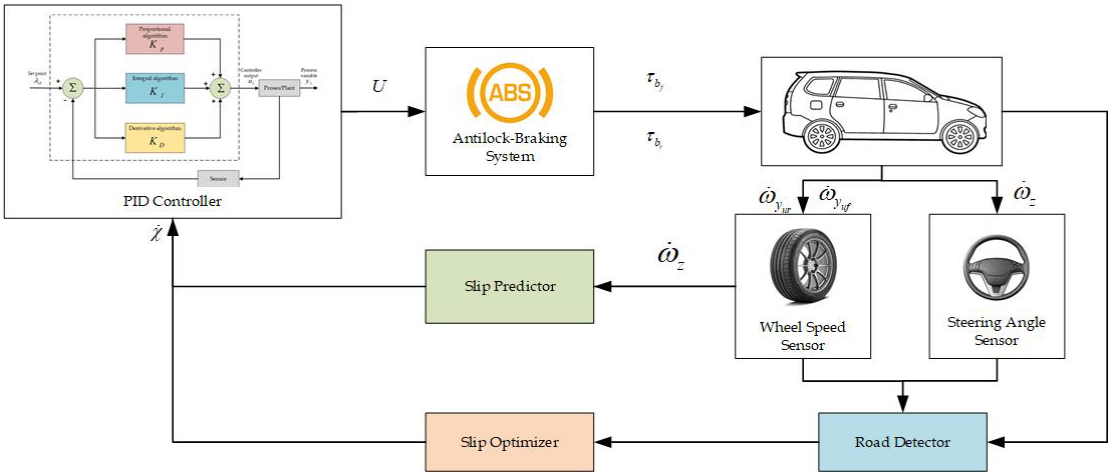

Fig. 7 *Single wheel braking model*

Table 2 *Single effect of K_P, K_i and K_d on system response*

Response	Rise time	Overshoot	Setting time	Steady state error
K_P	Decrease	Increase	Small effect	Decrease
K_i	Decrease	Increase	Increase	Gone
K_d	Small effect	Down	Decrease	Small effect

From the table above, the proportional controller will reduce the settling time, increase the maximum pass percentage, and reduce the steady state. Meanwhile, the derivative proportional controller reduces the overshoot and settling time. In addition, the integral proportional controller decreases with rise time, increasing the maximum pass and descent time and will eliminate state errors. The proportional control signal is directly proportional to the error signal, as indicated by Eq. (27).

$$u(t) = K_p e(t) \tag{27}$$

The PI and PID control signals are represented by Eq. (28) and Eq. (29).

$$u(t) = K_p \left(e(t) + \frac{1}{T_i} \int e(t)dt \right) \tag{28}$$

$$u(t) = K_p \left(e(t) \frac{1}{T_i} \int e(t)dt + T_d \frac{de(t)}{dt} \right) \tag{29}$$

The following relations are used to find the integral and derivative constants.

The integral gain is $K_i = \frac{K_p}{T_i}$; and the derivative gain is $K_d = K_p T_d$; where $K_p$is proportional gain, T_i and T_d are integral and derivative time respectively given in Table 3. The PID controller parameters are obtained by using Ziegler-Nichols closed loop method [7]. The values of (K_p), $(K_i)$and (K_d) are decided using any standard rule. .. The values of Kp, Ki, and Kd are determined according to the Ziegler-Nichols tuning rule. The value of critical gain K_{cr} and corresponding period $P_{cr}$are determined experimentally or can be calculated using bode plot.

Table 3 *Ziegler-nichols tuning rule*

Gain coefficient	PID
Proportional Gain (K_p)	0.6 K_{cr}
Integral Time (T_i)	0.5 P_{cr}
Derivative time (T_d)	0.125 P_{cr}

The implementation of this study was conducted using simulation of ABS which is a combination from vehicle speed, wheel speed and slip through MATLAB Simulink. For ABS (Antilock Braking System) simulation, several parameters can be used to model and analyze the behavior of the ABS system. Some common parameters may be included in Table 4.

Table 4 *Parameters used in simulation*

Parameter	Description	Value
m	Vehicle mass	1500 kg
m_{uf}	Unsprung mass in the front suspension	220 kg
m_{ur}	Unsprung mass in the rear suspension	250 kg
I_w	Moment of Inertia	1.2 kgm^2
r_w	Wheel radius	0.28 m
V_0	Initial Vehicle Velocity	25 m/s
g	Gravitational constant	9.81 m/s^2
T_b	Braking Torque	1500 Nm
l_f	Distance between centroid and front axles	1.52 m
l_r	Distance between centroid and rear axles	1.83 m
μ_{dry}	Coefficient of friction for dry road	0.8
μ_{wet}	Coefficient of friction for wet road	0.4

4. Results and Discussion

The Anti-lock Braking System (ABS) is a pivotal component in enhancing safety and enhancing control in the context of braking performance. Braking Distance: one significant aspect of braking performance is the distance a vehicle takes to come to a complete stop after the brakes are applied.

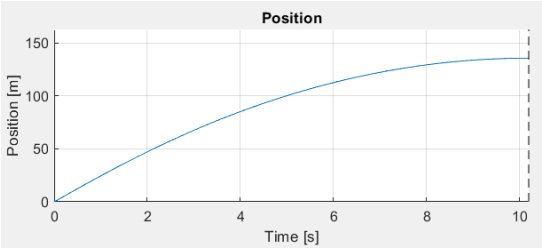

(a)

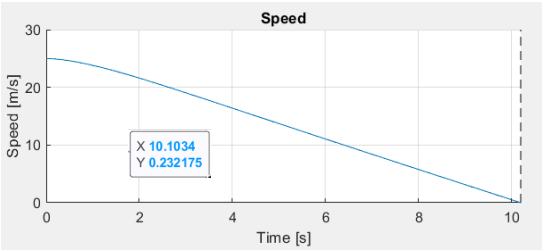

(b)

Int. Journal of Integrated Engineering Vol. 17 No. 5 (2025) p. 98-114

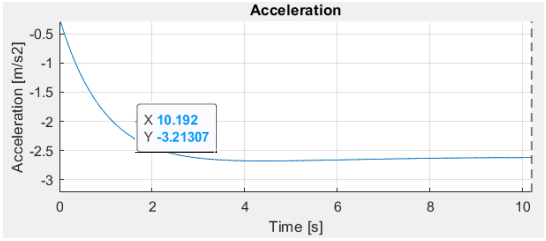

(c)

Fig. 8 *ABS braking performance without PID controller: (a) Position vs time; (b) Speed vs time; and (c) Acceleration vs time*

In the ABS braking performance without PID controller in Fig. 8, an abrupt deceleration occurring at a longitudinal displacement of 135 *m*, lasting for an estimated duration of 10 seconds. Upon the activation of sudden braking, the vehicle undergoes a reduction in its initial velocity from 25 *m/s* to a state of rest, a process that requires approximately 10 seconds to complete. This deceleration is achieved through the application of a braking acceleration measuring -3.2 m/s^2.

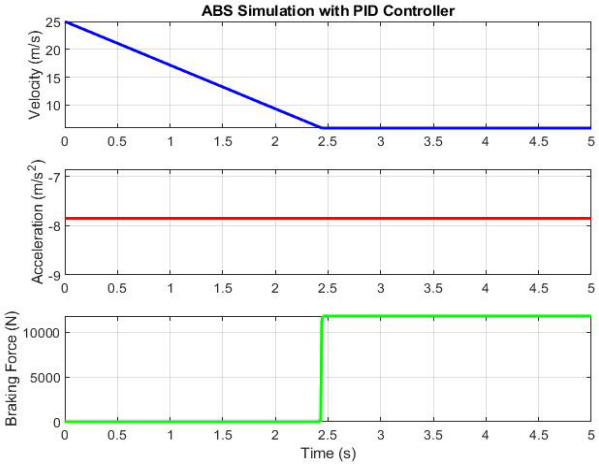

Fig. 9 *ABS braking performance using PID controller in dry road*

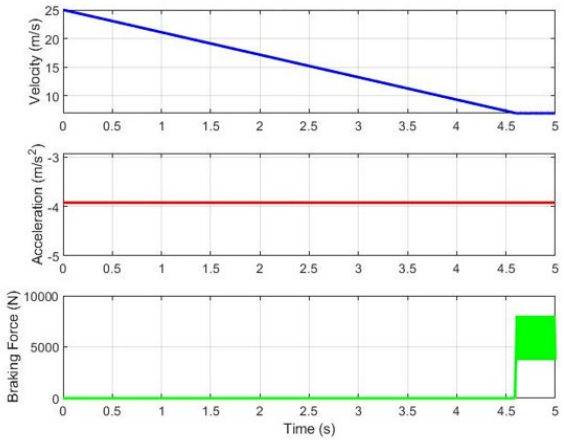

Fig. 10 *ABS braking performance using PID controller in wet road*

In Fig. 9, the vehicle experienced sudden braking in dry road at a vehicle velocity 25 *m/s* to a complete stop, which takes about 2.4 second with a braking force 12000 *N* and decrease the acceleration in 7.85 m/s^2. Besides that, in wet road conditions will take around 4.6 seconds to complete stop with a braking force of 8000 *N* and decrease the acceleration in 3.92 m/s^2 depict in Fig. 10.

This phenomenon above arises when the wheel undergoes a locking motion after the abrupt application of the braking force. When the wheels lose traction and experience wheel lock up, they cease to rotate. These issues have the potential to result in the driver's loss of control over the vehicle. In response to this issue, a safety mechanism was devised with the objective of mitigating the stopping distance by preventing wheel lock-up when braking. The system in question is commonly referred to as the Antilock Braking System (ABS).

A sprung mass that shown in Fig. 11 typically refers to the mass of a vehicle's body or any object supported by a spring or suspension system. In the result we find the velocity response with the settling time 2.0 *s*, overshoot value is 1.68, and the displacement response have a settling time 1.6 *s* with overshoot value 0.29. As the vehicle's wheels encounter changes in road conditions, such as bumps, potholes, or uneven surfaces, the unsprung mass reacts to these changes by displacing them vertically.

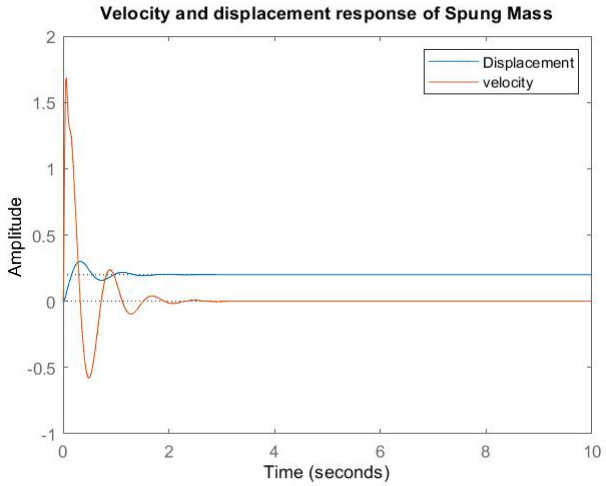

Fig. 11 *Velocity and displacement response of sprung mass*

In this instance, it is evident that the system experiences a more rapid stabilization, resulting in the cessation of oscillations that are known to adversely impact passenger comfort. The size of the displacement of the unsprung mass in Fig. 12, is mitigated the velocity response with the settling time 0.2 *s*, and overshoot value is 6.27, in the displacement have settling time response 0.06 s with overshoot value 0.24.

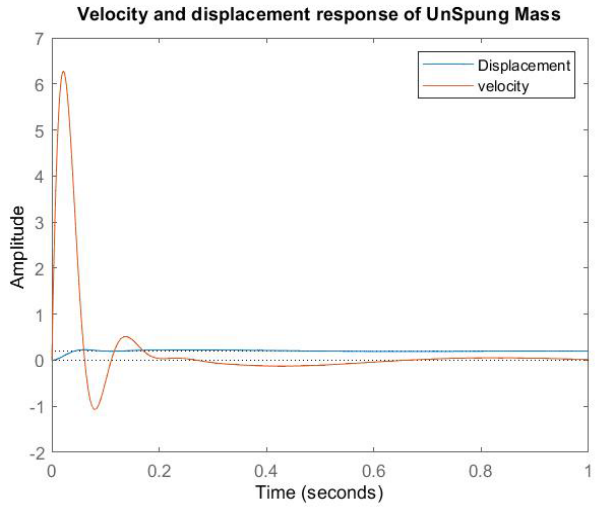

Fig. 12 *Velocity and displacement response of unsprung mass*

During braking, the vehicle's deceleration generates forces that act on both the sprung and unsprung masses. The ABS system modulates the braking pressure on in-dividual wheels to prevent them from locking up, allowing the wheels to maintain traction with the road surface. As the wheels slow down due to braking, the unsprung mass

Int. Journal of Integrated Engineering Vol. 17 No. 5 (2025) p. 98-114

responds to changes in the road surface and braking forces more quickly than the sprung mass. When the ABS is engaged, it modulates the brake pressure on individual wheels rapidly, creating a pulsing effect.

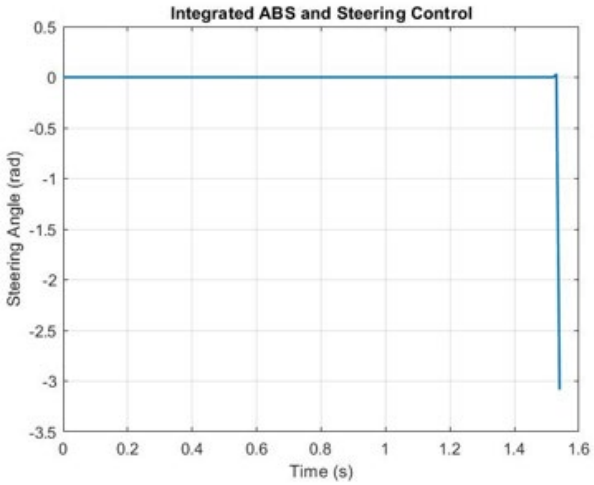

Fig. 13 *Steering angle during vehicle braking*

In Fig. 13, shown a negative steering angle. As the vehicle's weight shifts forward during braking, the front wheels bear a greater portion of the load, leading to an in-creased downward force on the front tires. This results in a phenomenon known as "negative steering angle" or "braking-induced steering." The negative steering angle means the front wheels tend to angle slightly inward (toward each other) by -3.2 rads at 1.57 seconds, causing the vehicle to veer slightly off its original path.

The integration of the Antilock Braking System (ABS) with the steering system in cars yields several significant findings. First, this integration effectively enhances vehicle control during emergency braking by synchronizing the responses of both systems. This coordination helps maintain stability, optimize braking force distribution, reduce the likelihood of wheel slip, and improve overall braking efficiency. The results also indicate that such integration minimizes braking distances, thereby improving the vehicle's responsiveness in critical situations. Additionally, the role of sensors in both ABS and steering systems is emphasized, as they provide accurate data essential for informed decision-making during braking events. These insights serve as a foundation for further advancements in integrated safety systems aimed at improving overall vehicle performance and safety.

5. Conclusion

The performance of the vehicle during emergency braking has significantly enhanced, exhibiting superior handling and characteristics when executing abrupt, high-speed maneuvers, accompanied by a simultaneous decrease in yaw-rate and sideslip angle. During the process of braking, several forces and moments come into play, resulting in changes in the direction of motion. When applying sudden and forceful pressure to the brakes, it is imperative to prioritize both maintaining vehicle stability and ensuring the ability to steer, in addition to achieving rapid deceleration. The consideration of variations in motion along the Z axis or the influence of yawing and rolling moments is not accounted for in our analysis. Subsequently, by utilizing the system's equations of motion, we may effectively regulate it using PID control. The implementation of system control is anticipated to mitigate the occurrence of abrupt vehicle locking, hence reducing the risk of overturning. This study also examined control performance through the implementation of a PID controller, which has the potential to enhance vehicle driving capabilities, safety measures, and operational stability. To ensure optimal vehicle direction stability, it is important to integrate the vehicle's control systems with other relevant components. The simulation results demonstrate the validation of the combined antilock-braking and steering system, indicating improved optimal braking distances and enhanced predictability. Furthermore, the findings indicate that the integrated control system surpasses the performance of the stand-alone braking and steering system.

Acknowledgement

This work was supported by LRI Universitas Muhammadiyah Yogyakarta under grant number 50/R-LRI/XII/2023. This work was also supported in part by Asia University, Taiwan, and China Medical University Hospital, China Medical University, Taiwan, under grant numbers below. ASIA-111-CMUH-16, ASIA-110-CMUH-22, ASIA108-CMUH-05, ASIA-106-CMUH-04, and ASIA-105-CMUH-04.

Conflict of Interest

Authors declare that there is no conflict of interests regarding the publication of the paper.

Author Contribution

Conceptualization: *H.-C.C. and A.W.;* ***Methodology:*** *H.-C.C. and A.W.;* ***Software:*** *A.W. and A.M.W.;* ***Validation:*** *H.-C.C. and A.W.;* ***Formal analysis:*** *A.W. and A.M.W.;* ***Investigation:*** *H.-C.C. and A.W.;* ***Resources:*** *A.W., C.-W.L. and A.M.W.;* ***Data curation:*** *A.W. and A.M.W;* ***Writing - original draft preparation:*** *H.-C.C. and A.W.;* ***Writing - review and Editing:*** *H.-C.C.;* ***Funding acquisition:*** *H.-C.C. and A.W. All authors have read and agreed to the published version of the manuscript.*

References

[1] Akmal Nizam Mohammed & Farzad Ismail (2013) Study of an entropy-consistent Navier-Stokes flux, *International Journal of Computational Fluid Dynamics, 27(1)*, 1-14, https://doi.org/10.1080/10618562.2012.752573

[2] Satria, R., Tsoi, K. H., Castro, M., & Loo, B. P. (2020). A combined approach to address road traffic crashes beyond cities: hot zone identification and countermeasures in Indonesia. *Sustainability*, *12*(5), 1801, https://doi.org/10.3390/su12051801

[3] Majid, M. A., Bakar, S. A., Mansor, S., Hamid, M. A., & Ismail, N. H. (2017). Modelling and PID value search for antilock braking system (ABS) of a passenger vehicle. *Journal of the Society of Automotive Engineers Malaysia*, *1*(3), 228-236, https://doi.org/10.56381/jsaem.v1i3.57

[4] Shao, J., Zheng, L., Li, Y. N., Wei, J. S., & Luo, M. G. (2007, August). The Integrated Control of Anti-lock Braking System and Active Suspension in Vehicle. In *2007 International Conference on Fuzzy Systems and Knowledge Discovery* (Vol. 4, pp. 519-523). IEEE Computer Society, https://doi.org/10.1109/FSKD.2007.571

[5] Aksjonov, A., Augsburg, K., & Vodovozov, V. (2016). Design and simulation of the robust ABS and ESP fuzzy logic controller on the complex braking maneuvers. *Applied Sciences*, *6*(12), 382, https://doi.org/10.3390/app6120382

[6] Aksjonov, A., Ricciardi, V., Augsburg, K., Vodovozov, V., & Petlenkov, E. (2020). Hardware-in-the-loop test of an open-loop fuzzy control method for decoupled electrohydraulic antilock braking system. *IEEE Transactions on Fuzzy Systems*, *29*(5), 965-975, https://doi.org/10.1109/TFUZZ.2020.2965868

[7] Rajendran, S., Spurgeon, S., Tsampardoukas, G., & Hampson, R. (2017). Time-varying sliding mode control for ABS control of an electric car. *IFAC-PapersOnLine*, *50*(1), 8490-8495, https://doi.org/10.1016/j.ifacol.2017.08.823

[8] Ivanov, V., Savitski, D., Augsburg, K., & Barber, P. (2015, March). Electric vehicles with individually controlled on-board motors: Revisiting the ABS design. In *2015 IEEE International Conference on Mechatronics (ICM)* (pp. 323-328). IEEE, https://doi.org/10.1109/ICMECH.2015.7083996

[9] Moaaz, A. O., Ali, A. S., & Ghazaly, N. M. (2020). Investigation of anti-lock braking system performance using different control systems. *International Journal of Control and Automation*, *13*(1s), 137-153.

[10] Gowda, D., Kumar, P., & BC, V. K. (2020, November). Dynamic analysis and control strategies of an anti-lock braking system. In *2020 4th International Conference on Electronics, Communication and Aerospace Technology (ICECA)* (pp. 1677-1682). IEEE. https://doi.org/10.1109/ICECA49313.2020.9297642

[11] Bera, T. K., Bhattacharya, K., & Samantaray, A. K. (2011). Evaluation of antilock braking system with an integrated model of full vehicle system dynamics. *Simulation Modelling Practice and Theory*, *19*(10), 2131-2150, https://doi.org/10.1016/j.simpat.2011.07.002

[12] Reif, K. (2014). Brakes, brake control and driver assistance systems. *Weisbaden, Germany, Springer Vieweg*, https://doi.org/10.1007/978-3-658-03978-3

[13] Vodovozov, V., Aksjonov, A., Petlenkov, E., & Raud, Z. (2021). Neural network-based model reference control of braking electric vehicles. *Energies*, *14*(9), 2373, https://doi.org/10.3390/en14092373

[14] Acosta Lúa, C., Di Gennaro, S., & Sánchez Morales, M. E. (2017). Nonlinear adaptive controller applied to an antilock braking system with parameters variations. *International Journal of Control, Automation and Systems*, *15*, 2043-2052, https://doi.org/10.1007/s12555-016-0136-1

[15] Gowda, D. V., & Ramachandra, A. C. (2017). Slip ratio control of anti-lock braking system with bang-bang controller. *International Journal of Computer Techniques*, *4*(1), 97-104,

[16] Wang, Z., Zhu, J., Zhang, L., & Wang, Y. (2018). Automotive ABS/DYC coordinated control under complex driving conditions. *IEEE access*, *6*, 32769-32779, https://doi.org/10.1109/ACCESS.2018.2834565

[17] Qin, Y., Wang, Z., Xiang, C., Hashemi, E., Khajepour, A., & Huang, Y. (2019). Speed independent road classification strategy based on vehicle response: Theory and experimental validation. *Mechanical Systems and Signal Processing*, *117*, 653-666, https://doi.org/10.1016/j.ymssp.2018.07.035

[18] Qin, Y., Langari, R., Wang, Z., Xiang, C., & Dong, M. (2017). Road excitation classification for semi-active suspension system with deep neural networks. *Journal of Intelligent & Fuzzy Systems*, *33*(3), 1907-1918, https://doi.org/10.3233/JIFS-161860

[19] Gowda, V. D., Ramachandra, A., Thippeswamy, M., Pandurangappa, C., & Naidu, P. R. (2019). Modelling and performance evaluation of anti-lock braking system. *Journal Engineering Science Technology*, *14*(5), 3028-3045,

[20] Zhang, W., Xu, G. N., Guo, X. X., Zhang, W., Wang, B., & Chen, M. (2015). PID and Velocity Feedback Control for ABS based on Wheel Slip. *Applied Mechanics and Materials*, *733*, 758-762, https://doi.org/10.4028/www.scientific.net/AMM.733.758

[21] Fu, Q., Zhao, L., Cai, M., Cheng, M., & Sun, X. (2012, April). Simulation research for quarter vehicle ABS on complex surface based on PID control. In *2012 2nd International Conference on Consumer Electronics, Communications and Networks (CECNet)* (pp. 2072-2075). IEEE. https://doi.org/10.1109/CECNet.2012.6201828

[22] Chen, C. P., & Chiang, M. H. (2018, June). Mathematical simulations and analyses of proportional electro-hydraulic brakes and anti-lock braking systems in motorcycles. In *Actuators* (Vol. 7, No. 3, p. 34). MDPI, https://doi.org/10.3390/act7030034

[23] Chindamo, D., Lenzo, B., & Gadola, M. (2018). On the vehicle sideslip angle estimation: a literature review of methods, models, and innovations. *Applied Sciences*, *8*(3), 355, https://doi.org/10.3390/app8030355

[24] Duan, C., Zheng, L., & Guo, X. (2021, December). The transformation method of vehicle dynamics right hand coordinate system and image left hand coordinate system. In *2021 International Conference on Information Technology and Biomedical Engineering (ICITBE)* (pp. 222-226). IEEE, https://doi.org/10.1109/ICITBE54178.2021.00056

[25] Cheng, Z., & Lu, Z. (2017). Nonlinear research and efficient parameter identification of magic formula tire model. *Mathematical Problems in Engineering*, *2017*(1), 6924506, https://doi.org/10.1155/2017/6924506

[26] Algadah, K. M., & Alaboodi, A. S. (2019). Anti-lock braking system components modelling. *Int. J. Innov. Technol. Explor. Eng*, *9*(2), 3969-3975, https://doi.org/10.35940/ijitee.B7248.129219

[27] Lu, F., Chen, S., & Zeng, Y. (2010, August). Modeling and simulation of four degree-of-freedom four-wheel-steering vehicle. In *2010 WASE International Conference on Information Engineering* (Vol. 3, pp. 104-108). IEEE, https://doi.org/10.1109/ICIE.2010.203

[28] Belrzaeg, M., Ahmed, A. A., Almabrouk, A. Q., Khaleel, M. M., Ahmed, A. A., & Almukhtar, M. (2021). Vehicle dynamics and tire models: An overview. *World Journal of Advanced Research and Reviews*, *12*(1), 331-348, https://doi.org/10.30574/wjarr.2021.12.1.0524

[29] Baarath, K., Zakaria, M. A., & Zainal, N. A. (2018). An investigation on the effect of lateral motion on normal forces acting on each tires for nonholonomic vehicle. In *Intelligent Manufacturing & Mechatronics: Proceedings of Symposium, 29 January 2018, Pekan, Pahang, Malaysia* (pp. 611-621). Springer Singapore, https://doi.org/10.1007/978-981-10-8788-2_55

[30] Oudghiri, M., Chadli, M., & El Hajjaji, A. (2007). Robust fuzzy sliding mode control for antilock braking system. *International Journal on Sciences and Techniques of Automatic Control*, *1*(1), 13-28,

[31] Ray, L. R. (1997). Nonlinear tire force estimation and road friction identification: Simulation and experiments. *Automatica*, *33*(10), 1819-1833, https://doi.org/10.1016/S0005-1098(97)00093-9

[32] Åström, K. J., & Hägglund, T. (2004). Revisiting the Ziegler–Nichols step response method for PID control. *Journal of process control*, *14*(6), 635-650, https://doi.org/10.1016/j.jprocont.2004.01.002

[33] O'dwyer, A. (2009). *Handbook of PI and PID controller tuning rules*. World Scientific.

[34] Boopathi, A. M., & Abudhahir, A. (2015). Firefly algorithm tuned fuzzy set-point weighted PID controller for antilock braking systems. *Journal of Engineering Research*, *3*, 1-16, https://doi.org/10.7603/s40632-015-0015-6

[35] Ziegler, J. G., & Nichols, N. B. (1942). Optimum settings for automatic controllers. *Transactions of the American society of mechanical engineers*, *64*(8), 759-765, https://doi.org/10.1115/1.4019264